

# DBZ is a putative PPAR $\gamma$ agonist that prevents high fat diet-induced obesity, insulin resistance and gut dysbiosis



Pengfei Xu<sup>a</sup>, Fan Hong<sup>a</sup>, Jialin Wang<sup>a</sup>, Jing Wang<sup>a,1</sup>, Xia Zhao<sup>c</sup>, Sheng Wang<sup>a</sup>, Tingting Xue<sup>a</sup>, Jingwei Xu<sup>d</sup>, Xiaohui Zheng<sup>e,\*</sup>, Yonggong Zhai<sup>a,b,\*\*</sup>

<sup>a</sup> Beijing Key Laboratory of Gene Resource and Molecular Development, College of Life Sciences, Beijing Normal University, Beijing 100875, China

<sup>b</sup> Key Laboratory for Cell Proliferation and Regulation Biology of State Education Ministry, College of Life Sciences, Beijing Normal University, Beijing, 100875, China

<sup>c</sup> Shijingshan Teaching Hospital of Capital Medical University, Beijing Shijingshan Hospital, Beijing, 100043, China

<sup>d</sup> Gene Engineering and Biotechnology Beijing Key Laboratory, College of Life Sciences, Beijing Normal University, Beijing, 100875, China

<sup>e</sup> Key Laboratory of Resource Biology and Biotechnology in Western China, College of Life Sciences, Northwest University, Xi'an, 710069, China

## ARTICLE INFO

### Keywords:

PPAR $\gamma$   
Obesity  
Insulin resistance  
Gut microbiota

## ABSTRACT

**Background:** The nuclear receptor PPAR $\gamma$  is an effective pharmacological target for some types of metabolic syndrome, including obesity, diabetes, nonalcoholic fatty liver disease, and cardiovascular disease. However, the current PPAR $\gamma$ -targeting thiazolidinedione drugs have undesirable side effects. *Danshensu Bingpian Zhi* (DBZ), also known as tanshinol borneol ester derived from *Salvia miltiorrhiza*, is a synthetic derivative of natural compounds used in traditional Chinese medicine for its anti-inflammatory activity.

**Methods:** *In vitro*, investigations of DBZ using a luciferase reporter assay and molecular docking identified this compound as a novel promising PPAR $\gamma$  agonist. Ten-week-old C57BL/6J mice were fed either a normal chow diet (NCD) or a high-fat diet (HFD). The HFD-fed mice were gavaged daily with either vehicle or DBZ (50 mg/kg or 100 mg/kg) for 10 weeks. The gut microbiota composition was assessed by analyzing the 16S rRNA gene V3 + V4 regions *via* pyrosequencing.

**Results:** DBZ is an efficient natural PPAR $\gamma$  agonist that shows lower PPAR $\gamma$ -responsive luciferase reporter activity than thiazolidinediones, has excellent effects on the metabolic phenotype and exhibits no unwanted adverse effects in a HFD-induced obese mouse model. DBZ protects against HFD-induced body weight gain, insulin resistance, hepatic steatosis and inflammation in mice. DBZ not only stimulates brown adipose tissue (BAT) browning and maintains intestinal barrier integrity but also reverses HFD-induced intestinal microbiota dysbiosis.

**Conclusions:** DBZ is a putative PPAR $\gamma$  agonist that prevents HFD-induced obesity-related metabolic syndrome and reverse gut dysbiosis.

**General significance:** DBZ may be used as a beneficial probiotic agent to improve HFD-induced obesity-related metabolic syndrome in obese individuals.

## 1. Introduction

Peroxisome proliferator activated receptors (PPARs) are a group of

nuclear receptors that includes PPAR $\alpha$ , PPAR $\beta/\delta$ , and PPAR $\gamma$ . These receptors play key roles in the regulation of cellular proliferation and differentiation, carbohydrate, lipid, and protein metabolism, and

**Abbreviations:** ACC, acetyl-CoA carboxylase; ADRB, adrenoreceptor beta; BAT, brown adipose tissue; CPT1 $\beta$ , carnitine palmitoyltransferase 1 beta; DBZ, danshensu bingpian zhi; Epi-WAT, epididymal white adipose tissue; FATP, fatty acid transport protein; FAS, fatty acid synthase; FFDS, fufang danshen; HFD, high-fat diet; HOMA-IR, homeostasis model index of insulin resistance; IGTT, intraperitoneal glucose tolerance test; IL-6, interleukin-6; ITT, insulin tolerance test; LDL-c, low-density lipoprotein cholesterol; LEfSe, linear discriminant analysis effect size; LPL, lipoprotein lipase; LPS, lipopolysaccharide; Mes-WAT, mesenteric white adipose tissue; NAFLD, nonalcoholic fatty liver disease; NCD, normal chow diet; NMDS, non-metric multidimensional scaling; ORO, oil red o; OTU, operational taxonomic unit; PCA, principal component analysis; PCoA, principal coordinate analysis; Per-WAT, perirenal white adipose tissue; PPAR $\gamma$ , peroxisome proliferator-activated receptor gamma; QUICKI, quantitative insulin check index; RDA, redundancy analysis; SREBP1c, sterol regulatory element binding protein 1c; T2D, type 2 diabetes; TC, total cholesterol; TCM, traditional Chinese medicine; TG, triglyceride; TLR, toll-like receptor; TNF $\alpha$ , tumor necrosis factor  $\alpha$ ; TZD, thiazolidinediones; UCP, uncoupling protein; WAT, white adipose tissue

\* Correspondence to: X. Zheng, College of Life Sciences, Northwest University, Xi'an, 710069, China.

\*\* Correspondence to: Y. Zhai, College of Life Sciences, Beijing Normal University, Beijing, 100875, China.

E-mail addresses: [Zhengxh@nwu.edu.cn](mailto:Zhengxh@nwu.edu.cn) (X. Zheng), [ygzhai@bnu.edu.cn](mailto:ygzhai@bnu.edu.cn) (Y. Zhai).

<sup>1</sup> Present address: Department of Biology Science and Technology, Baotou Teacher's College, Baotou 014030, China.

<http://dx.doi.org/10.1016/j.bbagen.2017.07.013>

Received 10 March 2017; Received in revised form 22 June 2017; Accepted 19 July 2017

Available online 20 July 2017

0304-4165/ © 2017 Elsevier B.V. All rights reserved.

metabolic homeostasis *in vivo* [1,2]. PPAR $\gamma$ , which is mainly present in adipose tissue, the intestine and macrophages, is well known for its role in regulating adipogenesis, insulin sensitivity, and inflammation [3]. Increasing evidence indicates that PPAR $\gamma$  is involved in the etiology and pathogenesis of numerous conditions associated with metabolic syndrome, including obesity, diabetes, NAFLD, and cardiovascular disease [4,5], making this receptor an attractive pharmacological target for the treatment and prevention of the above-mentioned metabolic disorders [6]. Currently, thiazolidinediones (TZDs), which are potent PPAR $\gamma$  agonists, are clinically effective for type 2 diabetes but can lead to serious side effects, such as congestive heart failure, edema, osteoporosis, weight gain and possibly bladder cancer [7]. Thus, the development of unique PPAR $\gamma$  partial agonists that are effective against metabolic syndrome but lack negative side effects is a promising approach.

In addition to the Human Microbiome Project and the National Microbiome Initiative launched in the United States, research on the microbiome is rapidly being pursued in the fields of health care, agriculture, industry and environmental science [8,9]. Microbes confer unique properties upon their hosts, and gut microbes affect many aspects of host metabolism and physiology [10]. Gut dysbiosis (also known as microbial imbalance) has been shown to affect the pathogenesis of many diseases, including obesity, diabetes, non-alcoholic fatty liver disease (NAFLD) [11], chronic fatigue syndrome, inflammatory bowel disease and cancer [12,13]. A high-fat diet (HFD) has been reported to cause gut dysbiosis (i.e. to increase the ratio of *Firmicutes* to *Bacteroidetes* at the phylum level) which is considered an etiopathogenesis of obesity and its related metabolic disorders [14–16]. Thus, reversing intestinal dysbiosis may protect against obesity development.

*Danshensu Bingpian Zhi* (DBZ), which is also known as tanshinol borneol ester [1,7,7-trimethylbicyclo[2.2.1]heptan-2-yl-3-(3,4-dihydroxyphenyl)-2-hydroxy-propanoate], is a synthetic derivative of natural compounds used in traditional Chinese medicine (TCM) formula *Fufang Danshen* (FFDS) [17,18]. The FFDS has been indicated to be effective on treating cardiovascular and cerebrovascular diseases for many years in China. DBZ is a novel synthetic compound that chemically links *Danshensu* (tanshinol) and *Bingpian* (borneol), and it has not been approved for clinical use in the patients. Whereas tanshinol is a natural compound derived from *Salvia miltiorrhiza*, that has been shown to exert various beneficial activities, including improvement of microcirculation and reduction of endothelial dysfunction and platelet aggregation [17,19]. *Fufang Danshen Diwan* (Compound Danshen Dripping Pills) has successfully completed phase 3 clinical trials in the United States (NCT01659580) for the treatment of chronic stable angina pectoris and ischemic heart disease [20]. We previously demonstrated that DBZ inhibited LPS-induced inflammation and macrophage lipid accumulation [17]. Preliminary pharmacological experiments showed that DBZ attenuated atherosclerosis in apolipoprotein E-deficient (ApoE<sup>-/-</sup>) mice (unpublished observations). Here, we investigated the metabolic influence of the unique PPAR $\gamma$  agonist DBZ on mice fed a HFD and evaluated whether its beneficial effects were related to the restoration of the normal gut microbiota.

## 2. Material and methods

### 2.1. Materials

DBZ was synthesized in Dr. Xiaohui Zheng's laboratory (Northwest University, China) and verified by liquid chromatograph-mass spectrometry (LC-MS) and nuclear magnetic resonance spectroscopy (purity: 99.6%) [17]. Lipopolysaccharides (LPS), troglitazone (Tro), pioglitazone (Pio), WY14643, GW1516 and GW9662 were obtained from Sigma-Aldrich (USA). Normal chow diet (NCD) and HFD (60% kcal from fat) were obtained from Beijing HFK Bioscience Co. Ltd. (China).

### 2.2. Cell culture and luciferase reporter assay

HEK 293 T and RAW264.7 cells were obtained from ATCC and maintained in Dulbecco's modified Eagle's medium (DMEM) and RPMI 1640 medium containing 10% fetal bovine serum (FBS, Biowest) and 1% penicillin-streptomycin, respectively. Dual luciferase assays were performed in 24-well plates with Lipofectamine 2000 transfection reagent (Invitrogen, USA) and measured using a Dual-Luciferase Reporter Assay Kit (Promega, USA) [17]. HEK 293 T cells were treated with DBZ (0–20  $\mu$ M) and transfected with pCMX-PPAR $\gamma$ , pCMX-PPAR $\alpha$  or pcDNA-hPPAR $\beta/\delta$  and PPRE  $\times$  3-TK-Luc. RAW264.7 cells were treated with Pio (10  $\mu$ M) or DBZ (0–20  $\mu$ M) and transfected with PPRE  $\times$  3-TK-Luc and were transiently transfected with NF- $\kappa$ B-Luc and co-treated with or without LPS (1  $\mu$ g/mL), DBZ (20  $\mu$ M), GW9662 (10  $\mu$ M), and pSP27/shPPAR $\gamma$  or pSP27/Mock. The shPPAR $\gamma$  and Mock sequences are listed in Supplementary Table 1 and the interference verification is shown in Supplementary Fig. 2. The pRL-TK construct was co-transfected as an internal control to verify the transfection efficiency. The results are representative of obtained from at least three replicate experiments.

### 2.3. Animals

All procedures were conducted according to the guidelines of the Ethics and Animal Welfare Committee of Beijing Normal University. Ten-week-old C57BL/6 J male mice (NCD:  $n = 6$ , HFD:  $n = 10$ , HFD + 50DBZ and HFD + 100DBZ:  $n = 12$  each, Vital River Laboratory Animal Technology Co. Ltd., China) were housed with 3–4 mice/cage, in a controlled environment (12-h light/dark cycle) with water and food available *ad libitum*. The DBZ groups HFD + 50DBZ and HFD + 100DBZ were fed a HFD and administered DBZ at doses of 50 or 100 mg/kg body weight (BW), respectively, by gavage once daily for 10 weeks. Intraperitoneal glucose tolerance tests (IGTTs) and insulin tolerance tests (ITTs) were performed at the 8th and 9th weeks using previously described methods [21]. Feces were collected at the end of the 10th week for subsequent analysis. The epididymal white adipose tissue (Epi-WAT), perirenal-WAT (Per-WAT), mesenteric-WAT (Mes-WAT), liver, brown adipose tissue (BAT) and gastrointestinal system were carefully collected, and weighted after sacrifice and then stored at  $-80^{\circ}\text{C}$ .

### 2.4. Histochemical and cytological evaluation

The Epi-WAT and BAT were fixed in 4% paraformaldehyde, embedded in paraffin, sectioned at 5- $\mu$ m thickness, and stained with hematoxylin and eosin (H&E) using standard procedures. For immunohistochemistry, BAT sections were incubated with an anti-uncoupling protein 1 (UCP1) antibody (Sigma, 1:100), followed by an anti-rabbit TRITC-labeled (EarthOx, 1:200) secondary antibody. Frozen liver sections (8–10  $\mu$ m) were stained with Oil Red O (ORO). Transwell migration assays were performed in 24-well plates containing polycarbonate membrane inserts (Corning); the migrated cells were stained with 0.1% Giemsa and quantified using ImageJ software [22]. The adipocyte sizes were analyzed using the Cell Profiler Software as previously described [23].

### 2.5. Biochemical analysis

Fasting blood samples were obtained from the orbital venous plexus of each mouse at the end of the experiment. The serum triacylglycerol (TG), total cholesterol (TC), and glucose levels and the liver TG levels were measured using commercially available kits (Applygen, China). The serum insulin, tumor necrosis factor  $\alpha$  (TNF $\alpha$ ) and interleukin-6 (IL-6) concentrations were measured using commercially available ELISA kits (Neobioscience, China). Insulin resistance was determined based on the homeostasis model index of insulin resistance (HOMA-IR:

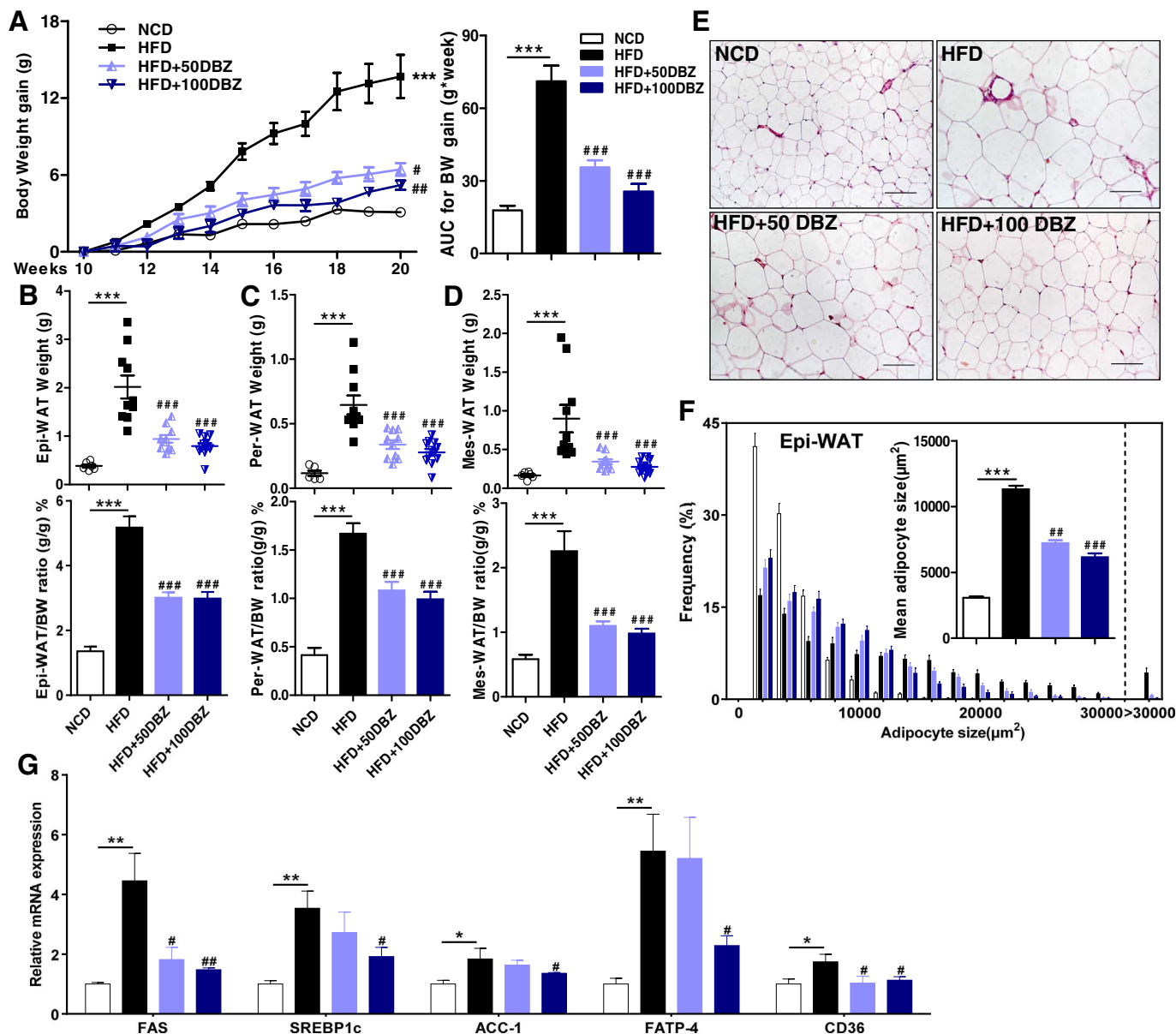


**Fig. 1.** DBZ decreases body weight gain and fat accumulation in mice fed a HFD. Effects of DBZ treatment (50 mg/kg/d or 100 mg/kg/d) on body weight gain and the calculated area under the curve AUC (A), the Epi-WAT weight and Epi-WAT/BW ratio (B), the Per-WAT weight and Per-WAT/BW ratio (C), and the Mes-WAT weight and Mes-WAT/BW ratio (D) in mice fed a NCD or a HFD for 10 weeks ( $n = 6-12$ ). (E) H & E staining of Epi-WAT sections (scale: 100  $\mu$ m). (F) Adipocyte size distribution and mean epididymal adipocyte size (inner) in each group ( $n = 5$  mice per group). (G) Relative mRNA expression of lipogenesis-related genes in the Epi-WAT was measured by real-time PCR analysis. Values are expressed as the mean  $\pm$  SEM. \* $P < 0.05$ ; \*\* $P < 0.01$ ; \*\*\* $P < 0.001$  compared with NCD/Con, # $P < 0.05$ ; ## $P < 0.01$ ; ### $P < 0.001$  compared with HFD.

insulin  $\times$  glucose / 22.5), and insulin sensitivity was calculated based on the quantitative insulin check index of insulin sensitivity (QUICKI:  $1 / [\log(\text{insulin}) + \log(\text{glucose})]$ ). The serum endotoxin content was measured using a quantitative chromogenic tachypleus amebocyte lysate kit (Chinese Horseshoe Crab Reagent Manufactory, China).

**2.6. Gene and protein expression analysis**

For quantitative real-time PCR analysis, total RNA was extracted from tissues using a RNeasy Pure Kit (Qiagen, China). Reverse transcription was performed using oligdT-18 and M-MLV transcriptase (Promega, USA). The assay was performed using SYBR Green qPCR SuperMix (Transgen Biotec, China) on an ABI 7500 real-time PCR system as described previously [22]. The primers used are listed in Supplementary Table 1. For the western blot analysis, tissue proteins were extracted using RIPA lysis buffer. Western blotting was performed

using standard procedures. The membranes were incubated with primary antibodies against toll-like receptor 4 (TLR-4) (1:1000), nuclear factor kappa B (NF- $\kappa$ B) (1:2000), UCP1 (1:5000) and  $\beta$ -actin (1:6000) followed by the appropriate secondary antibodies (EarthOx, 1:6000). The intensity of the protein bands was quantified using ImageJ.

**2.7. Molecular docking**

The three-dimensional structure of the ligand-binding domain of human PPAR $\gamma$  has been determined (Protein Data Bank, ID: 2VSR) [24]. The DBZ structure was built using Molecule Builder in MOE. The force field, receptor-ligand affinity, and reasonable binding models were analyzed using AutoDock. Predicted binding poses were visualized, and ligand-protein interactions were analyzed using PyMOL; the binding site was defined as a 6- $\text{\AA}$  sphere.

## 2.8. Gut microbiota profiling

Bacterial genomic DNA was isolated using a QIAamp DNA Mini Kit (Qiagen, Germany). The concentration and purity of the isolated DNA were monitored by electrophoresis on 1% agarose gels. Then the DNA was PCR amplified using specific bacterial primers (Supplementary Table 1) targeting the 16S rRNA V3 + V4 regions. A metagenomic sequencing library was generated using the Illumina MiSeq platform (Biomarker Technologies, China). The reads were merged using FLASH [25] and quality filtered using Trimmomatic [26]. The resulting sequences were grouped into operational taxonomic units (OTUs) based on sequence with a 97% threshold of similarity using UPARSE [27]. The alpha diversity analysis included OTU-Venn diagrams, the OUT number, Shannon index curves, the OTU rank, and rarefaction analysis; additionally, the Shannon, Chao 1, and Simpson indices were calculated. The beta diversity analysis included principal coordinate analysis (PCoA), principal component analysis (PCA), non-metric multi-dimensional scaling (NMDS), and the construction of a heatmap of the key OTUs identified in the redundancy analysis (RDA). These analyses were performed using QIIME [28]. Linear discriminant analysis effect size (LEfSe) analysis was used to quantify the biomarkers among groups of samples [29] with LDA values > 4.

## 2.9. Statistical analyses

Results are expressed as the means  $\pm$  SEM. Statistical analyses were performed using SPSS. Differences between groups were analyzed using ANOVA followed by Tukey's multiple comparison test or an unpaired Student's *t*-test and were considered significant at  $P < 0.05$ . The RDA was considered statistically significant at  $P < 0.01$ .

## 3. Results

### 3.1. DBZ prevents HFD-induced body weight gain

Using a mouse model of obesity, we observed that the HFD-induced a significant increase in body weight and in the Epi-WAT, Per-WAT, and Mes-WAT fat mass compared with mice fed the NCD. Compared with the vehicle-treated mice, treatment with DBZ (50 or 100 mg/kg/day) by gavage markedly prevented body weight gain and fat accumulation in the HFD-fed mice (Fig. 1A–D). Histological assessment of the Epi-WAT sections showed that the sizes of adipocytes were significantly decreased in the mice that received DBZ treatment and the HFD, reflecting an increased frequency of smaller adipocytes and a decreased frequency of larger adipocytes (Fig. 1E and F). As shown in Fig. 1G, DBZ treatment, especially at the higher dose (100 mg/kg/day), lowered the expression of lipogenic genes, including fatty acid synthase (FAS), sterol regulatory element binding protein 1c (SREBP1c), acetyl-CoA carboxylase (ACC-1), fatty acid transport protein 4 (FATP-4), and CD36.

### 3.2. DBZ improves HFD-induced insulin resistance and decreases liver steatosis and systemic low-grade inflammation

As obesity is closely related to insulin resistance, we measured the fasting blood glucose and serum insulin levels of the mice and calculated their QUICKI and HOMA-IR values according to previous formulas. As shown in Fig. 2A–D, DBZ treatment significantly improved insulin resistance in obese mice, restored normal serum fasting blood glucose and insulin concentrations, and nearly normalized the QUICKI and HOMA-IR indices. The IGTT and ITT results confirmed the beneficial effects of DBZ on insulin levels and glucose tolerance in HFD-fed mice (Fig. 2E–F). Next, we measured the serum and liver lipid contents. As shown in Fig. 2G–I, the serum and liver TG concentrations were significantly decreased in the DBZ-treated mice, whereas the serum TC concentration displayed little change. ORO staining of liver sections confirmed that DBZ inhibited lipid accumulation in the livers of the

obese mice (Fig. 2J). Because HFD-induced obesity, insulin resistance, and liver steatosis are strongly associated with low-grade chronic inflammation, we also tested the effects of DBZ on endotoxemia and the serum levels of inflammatory cytokines (TNF $\alpha$  and IL-6). As shown in Fig. 2K–M, DBZ supplementation reduced the serum endotoxin and TNF $\alpha$  concentrations to near-normal levels in the HFD fed mice. The occurrence of endotoxemia via the TLR-4 signaling pathways controls the production of pro-inflammatory factors in the liver and gives rise to the chronic inflammation associated with HFD-induced obesity [30]. DBZ administration suppressed TLR-4 and NF- $\kappa$ B protein expression in the liver compared with the untreated mice fed the HFD (Fig. 2N).

Taken together, these results show that DBZ treatment prevents HFD-induced obesity, insulin resistance, hepatic steatosis, and systemic low-grade inflammation.

### 3.3. DBZ blocks LPS-induced NF- $\kappa$ B activation and macrophage migration, partly by functioning as a PPAR $\gamma$ agonist

Previous studies have shown that DBZ mediates anti-inflammatory activity by inhibiting NF- $\kappa$ B [17] and that activation of PPAR $\gamma$  suppresses inflammation by maintaining co-repressors acting at the promoters of NF- $\kappa$ B target genes [31]. We speculated that the inhibition of NF- $\kappa$ B by DBZ resulted from PPAR $\gamma$  activation. The luciferase reporter assays showed that DBZ induced PPAR $\gamma$ -responsive luciferase reporter activity in HEK 293 T and RAW 264.7 cells (Fig. 3A). Meanwhile, DBZ had little activation on PPAR $\alpha$  and no effect on PPAR $\beta/\delta$  (Supplementary Fig. 1A and B). To examine whether the inhibition of NF- $\kappa$ B by DBZ depended on the PPAR $\gamma$  pathway, RAW264.7 cells were co-transfected with both NF- $\kappa$ B-responsive luciferase reporter genes and the shPPAR $\gamma$  plasmid or treatment with GW9662, a pharmacological inhibitor of PPAR $\gamma$ , followed treated with DBZ and then stimulated by LPS (1  $\mu$ g/mL). GW9662 mildly enhanced NF- $\kappa$ B activity in RAW264.7 cells (13.8%). As shown in Fig. 3B and C, compared with treatment with DBZ alone (20  $\mu$ M), co-treatment with shPPAR $\gamma$  or GW9662 restored NF- $\kappa$ B activity (36.4% and 41%, respectively). Moreover, co-treatment with GW9662 abrogated the inhibitory effect of DBZ on LPS-induced macrophage migration in RAW264.7 macrophages (Fig. 3D and E).

To further characterize the interaction of DBZ with PPAR $\gamma$ , we performed a molecular docking analysis. The docking results showed that DBZ could fit into the ligand-binding pocket of human PPAR $\gamma$  (Fig. 3F). Additionally, the hydrogen bonds at Glu291 and Ser342 (potential) and hydrophobic interactions at Met348 and Ile281 maintained the binding stability (Fig. 3G). Collectively, these data show that DBZ abrogates LPS-induced NF- $\kappa$ B activation and macrophage migration, partly through the activation of PPAR $\gamma$ .

### 3.4. DBZ alters the BAT and intestinal morphology of in HFD-fed mice

BAT is a highly active metabolic tissue that regulates energy expenditure and reduces obesity [32]. As observed in Fig. 4A, BAT from the HFD mice contained some large lipid droplets, which is a typical feature of the so-called whitening of BAT in response to a HFD challenge. DBZ treatment resulted in smaller lipid droplets and increased UCP1 protein expression in the BAT (Fig. 4B). Gene expression analysis showed that DBZ treatment increased the expression of genes involved in mitochondrial biogenesis and thermogenesis (PGC1 $\alpha$ , UCP1, UCP2, and adrenoreceptor beta 3(ADRB3)), fatty acid uptake (CD36 and FABP4), and fatty acid catabolism (lipoprotein lipase (LPL) and carnitine palmitoyltransferase 1 beta (CPT1 $\beta$ )) (Fig. 4C–J).

Recent studies have shown that the small intestines of animals fed a HFD are shorter in length, weigh less, and have decreased intestinal permeability compared with those of animals fed a NCD [33,34]. DBZ administration led to a significant increase in the intestinal length (Fig. 5A). Furthermore, the main increase in length occurred in the small intestine rather than in the colon (Fig. 5B and C). We weighed different segments of the gastrointestinal tract (stomach, small

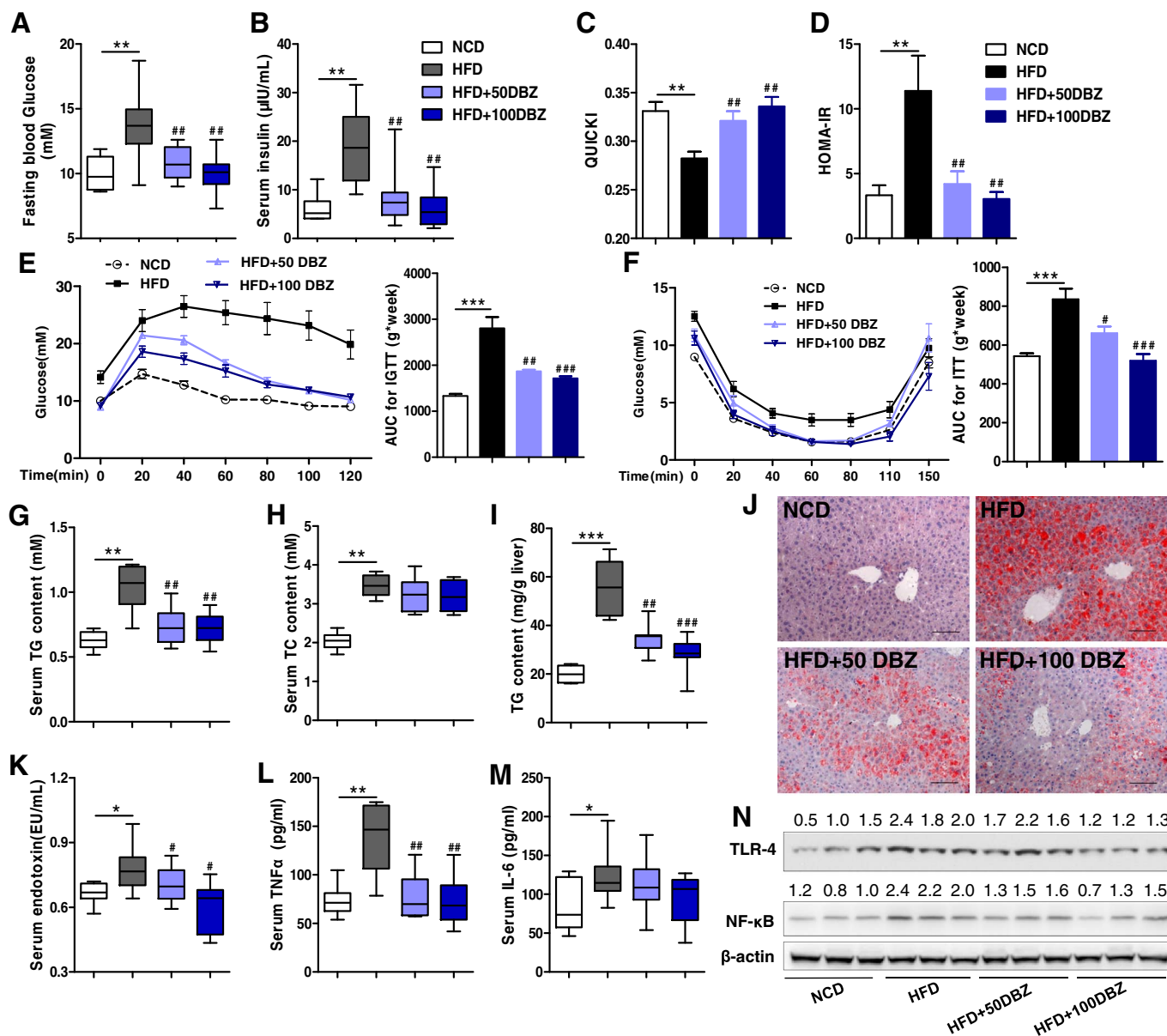


**Fig. 2.** DBZ prevents HFD-induced insulin resistance, hepatic steatosis, and systemic inflammation. Serum concentrations of fasting blood glucose (A), insulin (B) and the calculated QUICKI (C) and HOMA-IR (D) in the mice shown in Fig. 1. (E) IGTT and (F) ITT results showing the curves of the blood glucose levels and the calculated AUCs (right). The serum TG (G), TC (H), endotoxin (K), TNFα (L) and IL-6 concentrations (M) and liver TG content (I) measured using relevant kits. (J) ORO staining of frozen liver sections (scale: 100 μm). (N) Liver TLR-4 and NF-κB protein production was examined by Western blotting, and the relative protein levels (indicated above by the bands) were normalized to β-actin. Values are expressed as the mean ± SEM (n = 6–12). \*P < 0.05; \*\*P < 0.01; \*\*\*P < 0.001 vs. NCD, #P < 0.05; ##P < 0.01; ###P < 0.001 vs. HFD.

intestine, cecum, and colon) and normalized them to the mouse BW. As shown in Fig. 5D–H and Supplementary Fig. 3A–E, the gastrointestinal tract, especially the cecum, weighed more in the DBZ-treated groups. Morphologically, feeding the animals with HFD led to a notable reduction in the villus length in the proximal jejunum, whereas treatment with DBZ normalized the villus length (Fig. 5I and J). As expected, DBZ treatment caused gene expression of the tight junction protein occludin to revert to a near-normal level (Fig. 5K).

### 3.5. DBZ modulates the gut microbiota composition in HFD-fed mice

The gut microbiota composition is linked to obesity and its related metabolic disorders. Therefore, we evaluated the effects of DBZ treatment on the gut microbiota by sequencing the bacterial 16S rRNA (V3 + V4 region) gene. In total, 1,103,762 clean tags (Supplementary Table 2) and 570 OTUs were obtained. The OTU-Venn and OTU number

illustrated the differences among groups (Fig. 6A and Supplementary Fig. 4A). The Shannon curves, OTU rank abundance, rarefaction curves and Shannon, Chao 1, and Simpson indices showed that the HFD-fed group displayed no significant differences in richness compared with the NCD-fed group, and that DBZ treatment (at 50 mg/kg/day) resulted in a mild decrease in the richness of the gut microbiota (Fig. 6B and Supplementary Fig. 4B–E). The UniFrac PCoA, NMDS, and PCA revealed distinct clustering of the microbiota composition in each group, with the DBZ treatment groups showing microbial compositions similar to the HFD groups (Fig. 6C and Supplementary Fig. 4F–G). The phylum level analysis showed that the HFD-fed mice had a significantly increased *Firmicutes* to *Bacteroidetes* ratio compared with the NCD-fed mice, whereas DBZ treatment increased the relative abundance of *Bacteroidetes* and decreased the relative abundance of *Firmicutes*, thereby reducing the *Firmicutes* to *Bacteroidetes* ratio (Fig. 6D). Similar results were observed upon assessing the details of each sample at the

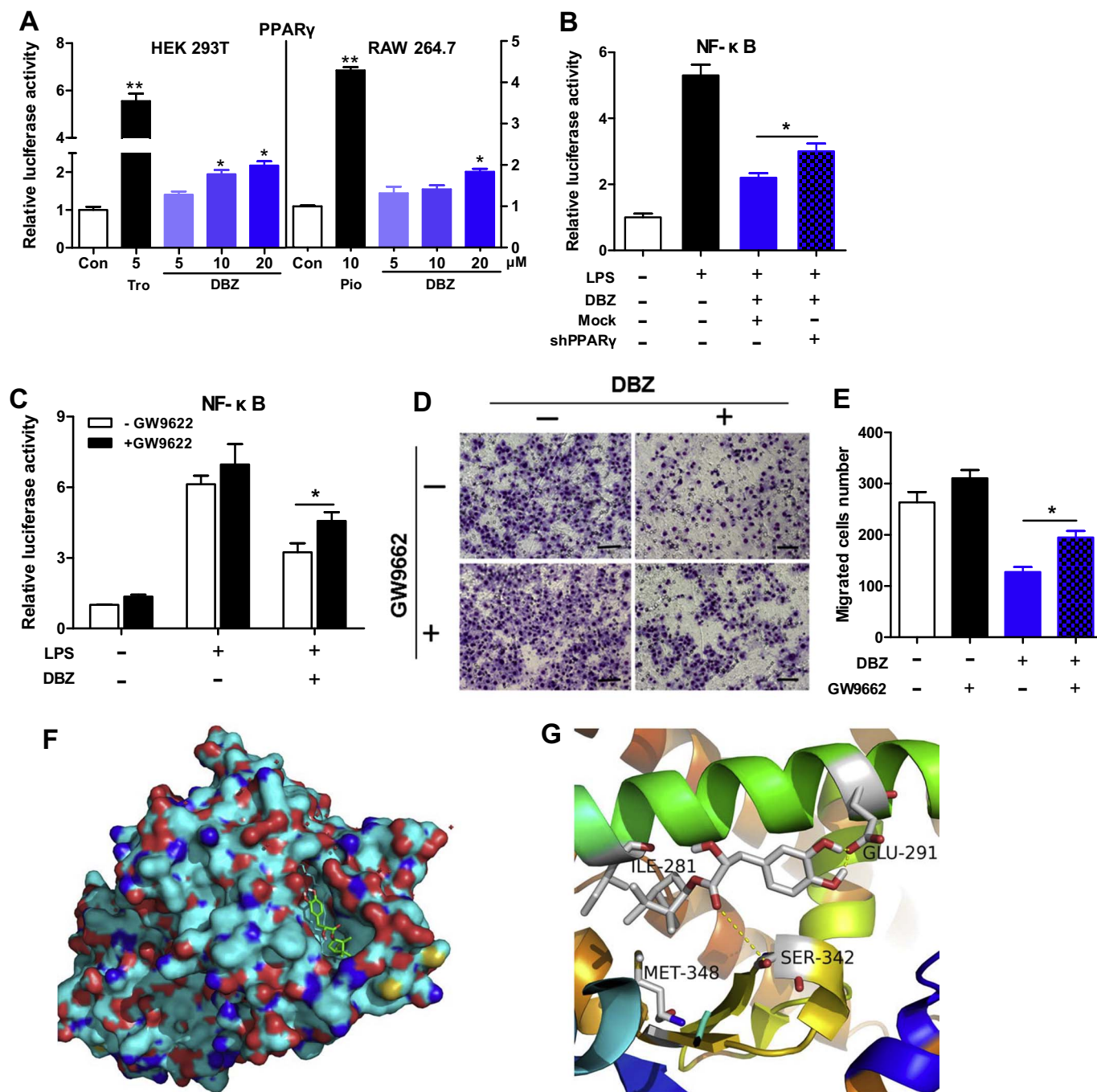


**Fig. 3.** DBZ blocks LPS-induced NF-κB activation and macrophage migration by activating PPAR $\gamma$ . (A) The transcriptional activity of PPAR $\gamma$  was assessed using transactivation reporter assays in HEK293T and RAW 264.7 cells treated with the indicated DBZ concentrations (5–20  $\mu$ M). Tro and Pio were induced as positive controls. The effect of DBZ (20  $\mu$ M) on LPS-induced NF-κB activation was assessed using a transactivation reporter assay in RAW264.7 cells after under knockdown with shPPAR $\gamma$  (B) or inhibition of PPAR $\gamma$  with GW9662 (C). GW9662 is a PPAR $\gamma$  inhibitor. The RAW264.7 cells were pre-treated with or without GW9662 and DBZ (20  $\mu$ M) for 24 h and then incubated with LPS (1  $\mu$ g/mL) for 6 h. Transwell assay to assess the effect of DBZ on LPS-induced macrophage migration. Representative images (D) and quantification (E) of the migrated cells are shown (scale: 50  $\mu$ m). (F, G) Model structure showing the complex formed by the PPAR $\gamma$  ligand-binding pocket and DBZ based on molecular docking. Data are presented as the mean  $\pm$  SEM from three independent experiments. \* $P$  < 0.05, \*\* $P$  < 0.01.

genus level (Fig. 6E). Strikingly, DBZ supplementation at 100 mg/kg/day resulted in a significant increase in *Akkermansia*, which are beneficial bacteria belonging to phylum *Verrucomicrobia*. The LefSe analysis was used to show the marker taxa of each group (Supplementary Fig. 5). As shown in Fig. 6F–I, DBZ treatment increased the levels of the intestinal mucin-degrading bacteria *Akkermansia*, which are considered probiotics that prevent the development of obesity, diabetes and inflammation, and suppressed HFD-induced pernicious bacteria, including *Helicobacter marmotae*, *Odoribacter*, and *Anaerotruncus*.

The RDA identified gut microbiota phylotypes whose abundances were changed by DBZ treatment (HFD vs HFD + 50DBZ or HFD vs HFD + 100DBZ). As shown in Fig. 7 and Supplementary Data 1, 121 predictive OTUs differed dramatically between the HFD group and each of the DBZ treatment groups ( $P$  < 0.01). In the HFD-fed mice, treatment with 50 or 100 mg/kg/day DBZ altered 48 (37 decreased and 11 increased), and 36 OTUs (31 decreased and 5 increased), respectively. All the decreased OTUs were toward to the same direction of NCD-fed mice. Taken together, these results suggested that DBZ supplementation

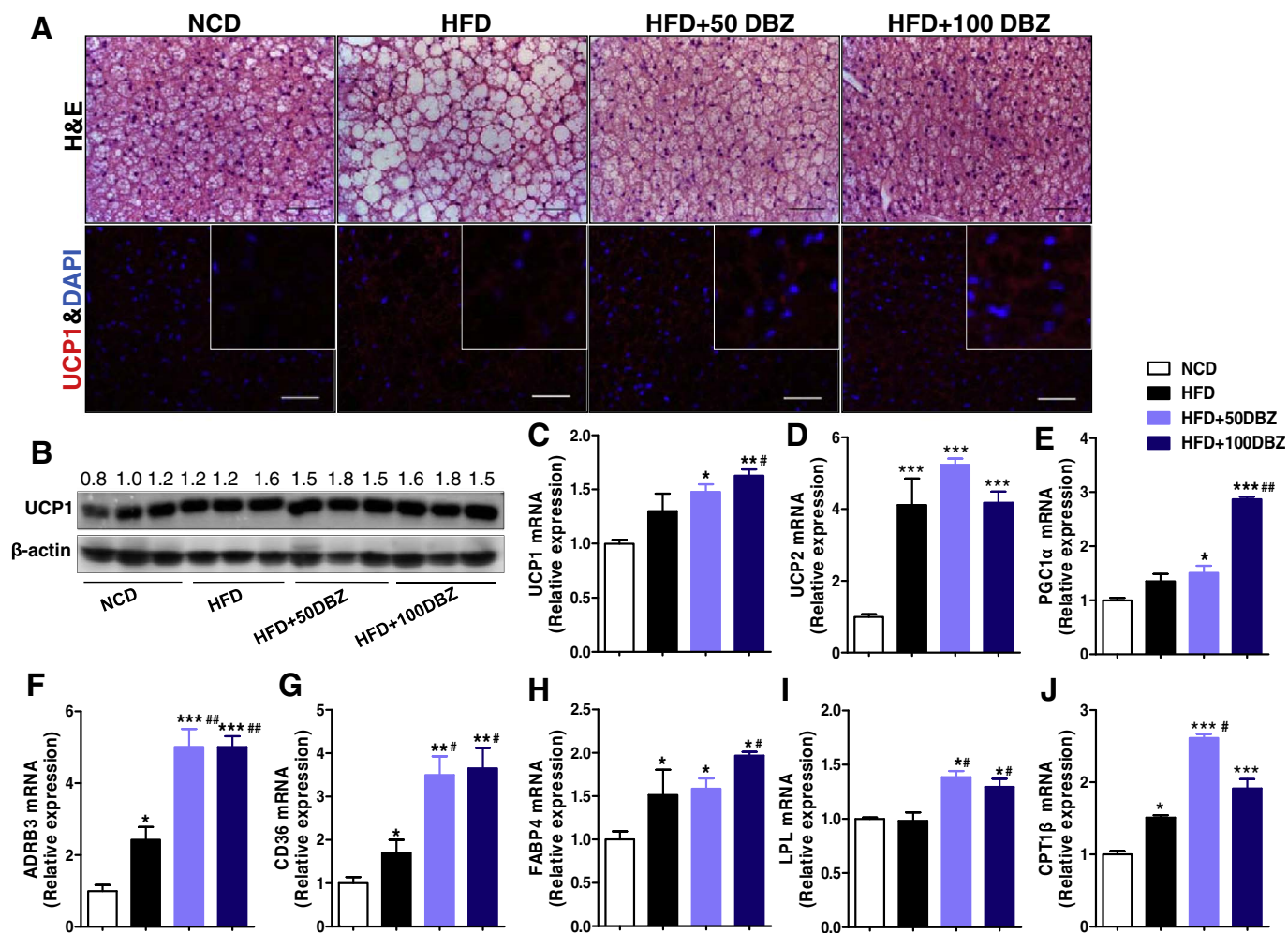


Fig. 4. Effects of DBZ on BAT browning in HFD-fed mice. (A) H & E and UCP1 immunofluorescence staining of representative BAT sections from mice in each group (scale: 50 μm). (B) UCP1 protein expression in the BAT was examined by western blotting. (C–J) Relative mRNA expression levels of genes involved in energy expenditure and thermogenesis in BAT. Values are expressed as the mean ± SEM (n = 3). \*P < 0.05; \*\*P < 0.01; \*\*\*P < 0.001 vs. NCD, #P < 0.05; ##P < 0.01 vs. HFD.

corrected the gut dysbiosis in obese mice.

#### 4. Discussion

Several previous studies have shown that DBZ inhibits LPS-induced inflammation and lipid accumulation in macrophages and decreases the TC, TG, and low-density lipoprotein cholesterol (LDL-c) levels and even atherosclerosis in rats [17,35]. In the present study, we evaluated the effects of DBZ administration at doses of 50 and 100 mg/kg/day for 10 weeks on the development of HFD-induced obesity and metabolic disorders and the composition of the gut microbiota in mice. Our results showed that DBZ treatment prevented obesity and its related metabolic disorders. Mechanistically, the metabolic benefits of DBZ administration may be explained by the inhibition of inflammation, browning of the BAT, restoration of intestinal barrier integrity and reversal of gut dysbiosis.

Recent reports have suggested that natural compound activators of PPARγ can improve metabolic syndrome and type 2 diabetes *in vivo* and have fewer side effects than potent synthetic PPARγ agonists (TZDs). For example, amorphastilbol was shown to improve glucose and lipid metabolism and was used successfully to treat diabetes and related metabolic disorders, including obesity and hepatomegaly, in *db/db* mice [36]. Honokiol reduced body weight gain and prevented hyperglycemia in diabetic KKAy mice [7]. Amorphrutins (amorphrutin 1 and amorphrutin B) markedly improved insulin and glucose tolerance and

other metabolic parameters without concomitant fat storage in the WAT and liver in diet-induced obese and *db/db* mice [37,38]. Here, the putative PPARγ agonist DBZ showed lower PPARγ-responsive luciferase reporter activity than troglitazone and pioglitazone, had excellent effects on the metabolic phenotypes and exhibited no unwanted adverse effects in our obese mouse model. What's more, we demonstrated DBZ attenuated atherosclerosis in *ApoE*<sup>-/-</sup> mice, and attenuated ox-LDL-induced foam cell formation and promoted cholesterol efflux in macrophages, likely through the activation of LXRα (unpublished observations). These results revealed that DBZ has pleiotropic effects in lipid and glucose metabolism through lipid metabolic nuclear receptors.

BAT maintains thermoregulation in newborns and is the main organ involved in non-shivering thermogenesis in mammals. BAT activity enhances thermogenesis from glucose and lipids, thereby protecting against obesity and chronic metabolic disease, including diabetes, dyslipidemia, atherosclerosis, and NAFLD [39,40]. In our previous study, we found melatonin stimulated BAT browning, and it might be associated with gut microbiota [41]. As shown in Fig. 4, DBZ reshaped the brown fat by increasing the mRNA and protein levels of the brown adipocyte marker UCP1 and enhancing lipid uptake into the BAT and thermogenesis. The PPAR family plays key roles in BAT adipogenesis and functions *via* recruiting diverse cofactors [42]. DBZ activates PPARγ transcriptional activity and may contribute to the beneficial phenotype in the BAT in cooperation with PGC1α.

Gut dysbiosis is closely related to obesity, diabetes, and NAFLD

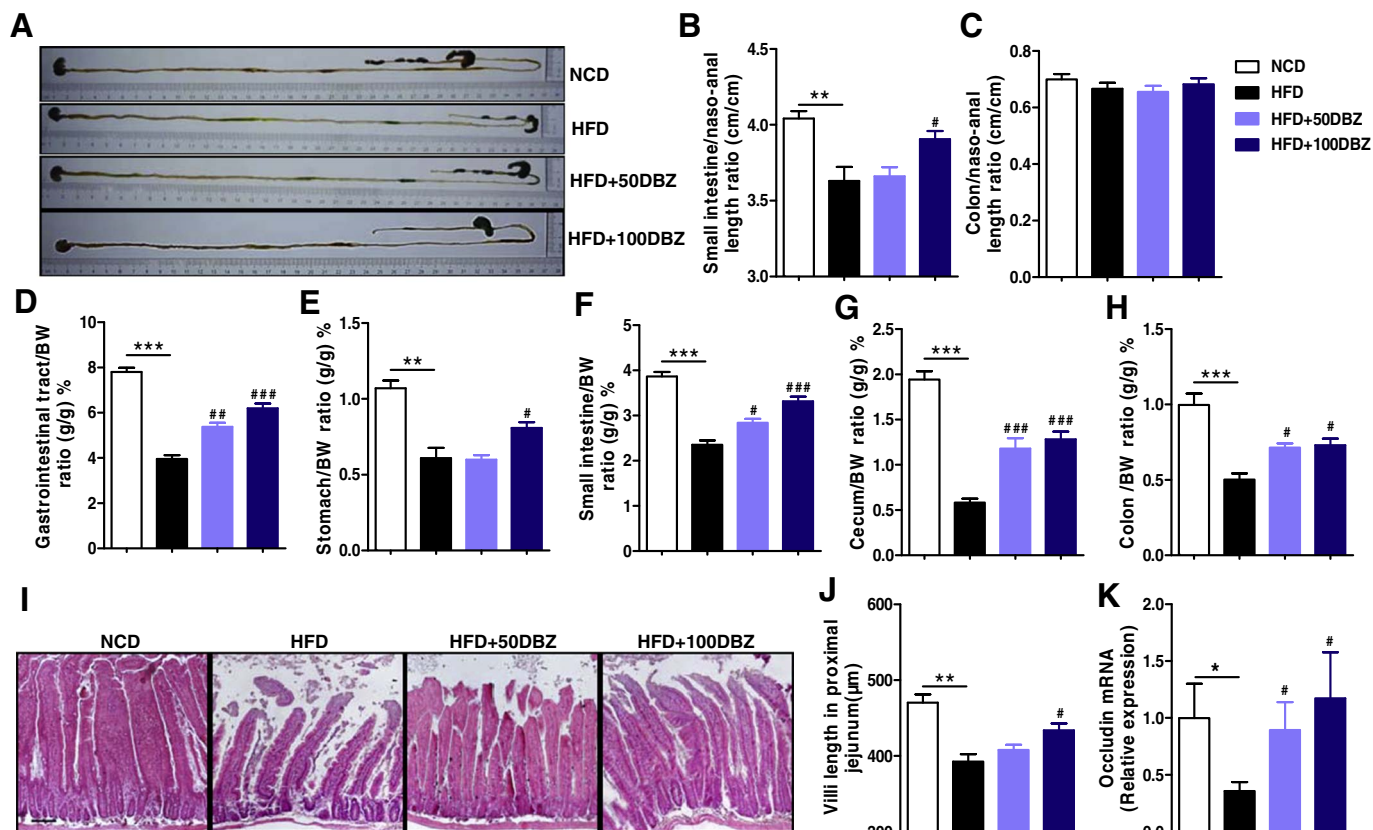


**Fig. 5.** DBZ alters the intestinal morphology in HFD-fed mice. (A) Representative images of the gastrointestinal system. The small intestine/naso-anal length ratio (B), colon/naso-anal length ratio (C), gastrointestinal tract/BW ratio (D), stomach/BW ratio (E), small intestine/BW ratio (F), cecum/BW ratio (G), and colon/BW ratio (H) in the mice are noted as outlined in Fig. 1. (I) H & E staining of proximal jejunum sections from the intestine as described in (A) (scale: 100  $\mu$ m). (J) Proximal jejunum villus lengths. (K) The ileum mRNA expression of occludin was measured by real-time PCR. Values are expressed as the mean  $\pm$  SEM ( $n = 6-12$ ). \* $P < 0.05$ ; \*\* $P < 0.01$ ; \*\*\* $P < 0.001$  vs. NCD, # $P < 0.05$ ; ## $P < 0.01$ ; ### $P < 0.001$  vs. HFD.

[43,44]. High fat diet and obesity relate to a specific gut dysbiota, which is enriched in *Firmicutes* and lack of *Bacteroidetes*. Gut microbiota can also play role in the development of diabetes and NAFLD, in part, increased the endotoxemia and activation of the TLR-4 signaling cascade [43]. And some specific microbiota such as *Akkermansia muciniphila* might be decreased in diabetes and when administered to mice exerted antidiabetic effects [44]. Therefore, the intestinal microbiota represents a novel therapeutic target for the treatment of these metabolic disorders. Measurement of the effects of DBZ supplementation on the gut microbiota can provide insights into the mechanism by which DBZ exerts its anti-obesity and anti-diabetic effects. As shown in Fig. 6, DBZ treatment notably increased the abundance of *Bacteroidetes* and reduced the abundance of *Firmicutes*, and then decreased the *Firmicutes* to *Bacteroidetes* ratio in the HFD-fed mice. DBZ meanwhile resulted in a higher relative abundance of *Akkermansia* compared with the mice that received a HFD alone. The mucin-degrading bacteria *Akkermansia* reside in the mucus layer of the intestine, where they help maintain a healthy mucosa [45,46]. In rodents and humans, the abundance of these bacteria is inversely correlated with diabetes and overweight [47,48]. Treatment with live *Akkermansia* protects against diet-induced obesity and intestinal barrier dysfunction in mice [49]. As shown in Fig. 5, DBZ alters the intestinal morphology and restores intestinal permeability, which is related to the presence of *Akkermansia* to some extent. Serum endotoxin mainly originates from the gut microbiota and is the primary agent of low-grade inflammation [50]. DBZ decreases intestinal permeability, thereby preventing the transfer of endotoxins from the gut to the circulatory system. DBZ treatment reduced the endotoxemia, suppressed TLR-4 signaling cascade, and then alleviated systemic low-grade inflammation. That association is, in part, due to

the changes in host intestinal morphology and microbial ecology. *Helicobacter marmotae* [51] is thought to cause enterohepatic disease in A/J mice. *Odoribacter* [52] and *Anaerotruncus* [45] were positively associated with obesity and glucose tolerance in diet-induced obese mice and type 2 diabetic db/db mice, and *Anaerotruncus* [52] was negatively correlated with the cecum weight. In the present study, the levels of these species were reversed by DBZ treatment in HFD-fed mice, which was consistent with the animals' phenotypes and metabolic parameters. The specific mechanism needs further research. Meanwhile, we should note that it is unclear whether DBZ treatment can alter gut microbiota under a normal diet and the change of gut microbiota composition is not strictly concentration-dependent under the high fat diet.

In summary, we found that DBZ, which is a natural compound derivative and a putative PPAR $\gamma$  agonist, protects mice against HFD-induced obesity, insulin resistance, hepatic steatosis, and low-grade systemic inflammation. DBZ also modulates gut microbiota dysbiosis by increasing *Bacteroidetes* to *Firmicutes* ratio, increasing the relative abundance of *Akkermansia*, and reducing the levels of the harmful bacterium *Helicobacter marmotae*. It is hoped that DBZ can be used as a therapeutic agent, or it represent a novel pharmacophore to develop novel therapeutic agents for the treatment of metabolic diseases.

**Author contributions**

Y.Z. and P.X. contributed to the study design; Y.Z. obtained funding; Z.X. provided the DBZ; P.X., J.W., F.H., S.W., and T.X. performed the experiments; P.X., F.H., J.W., and X.Z. analyzed the data; J.X. performed the docking assay; P.X. wrote the manuscript. Y.Z. and Z.X. determined the final content of this manuscript. All authors reviewed

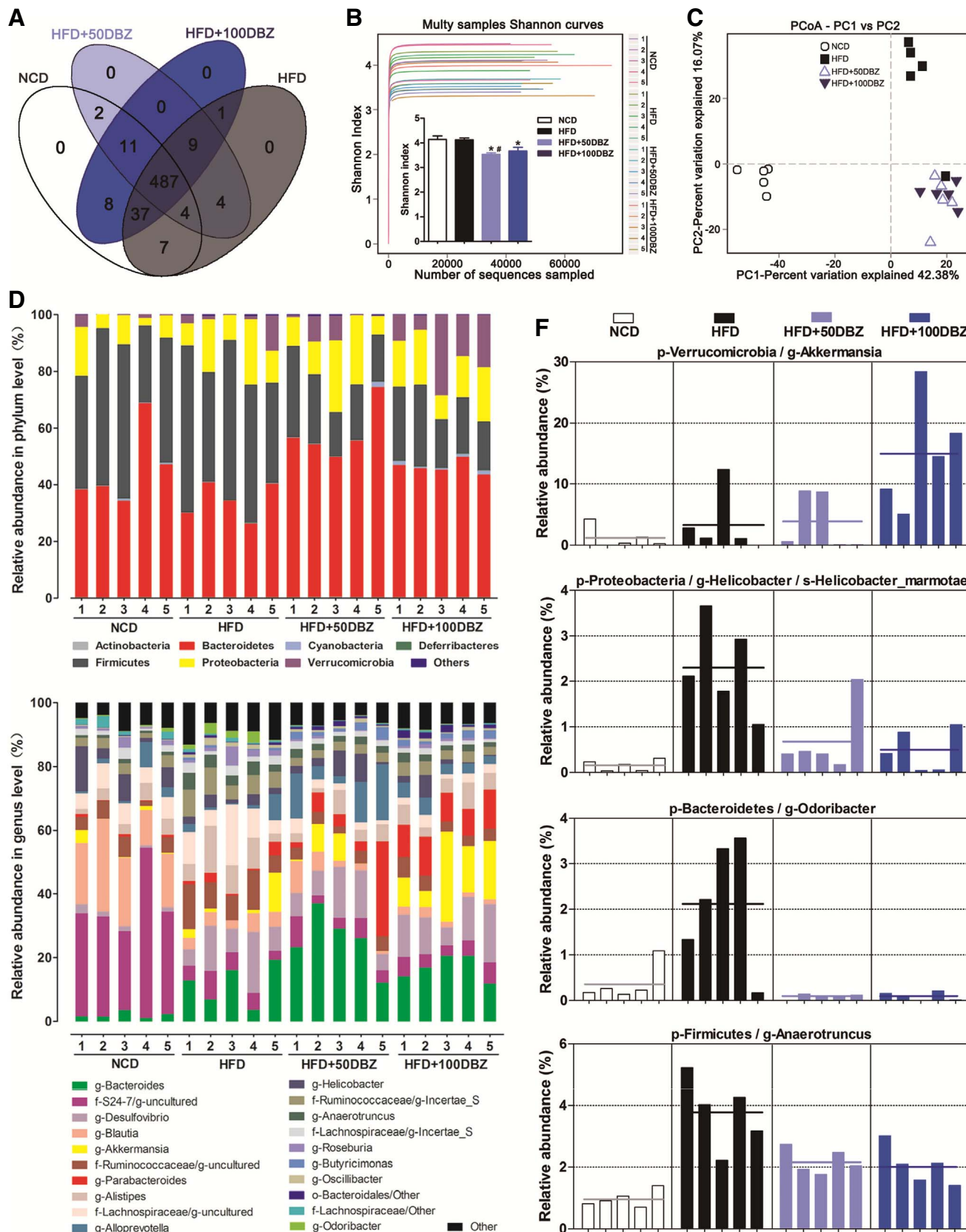
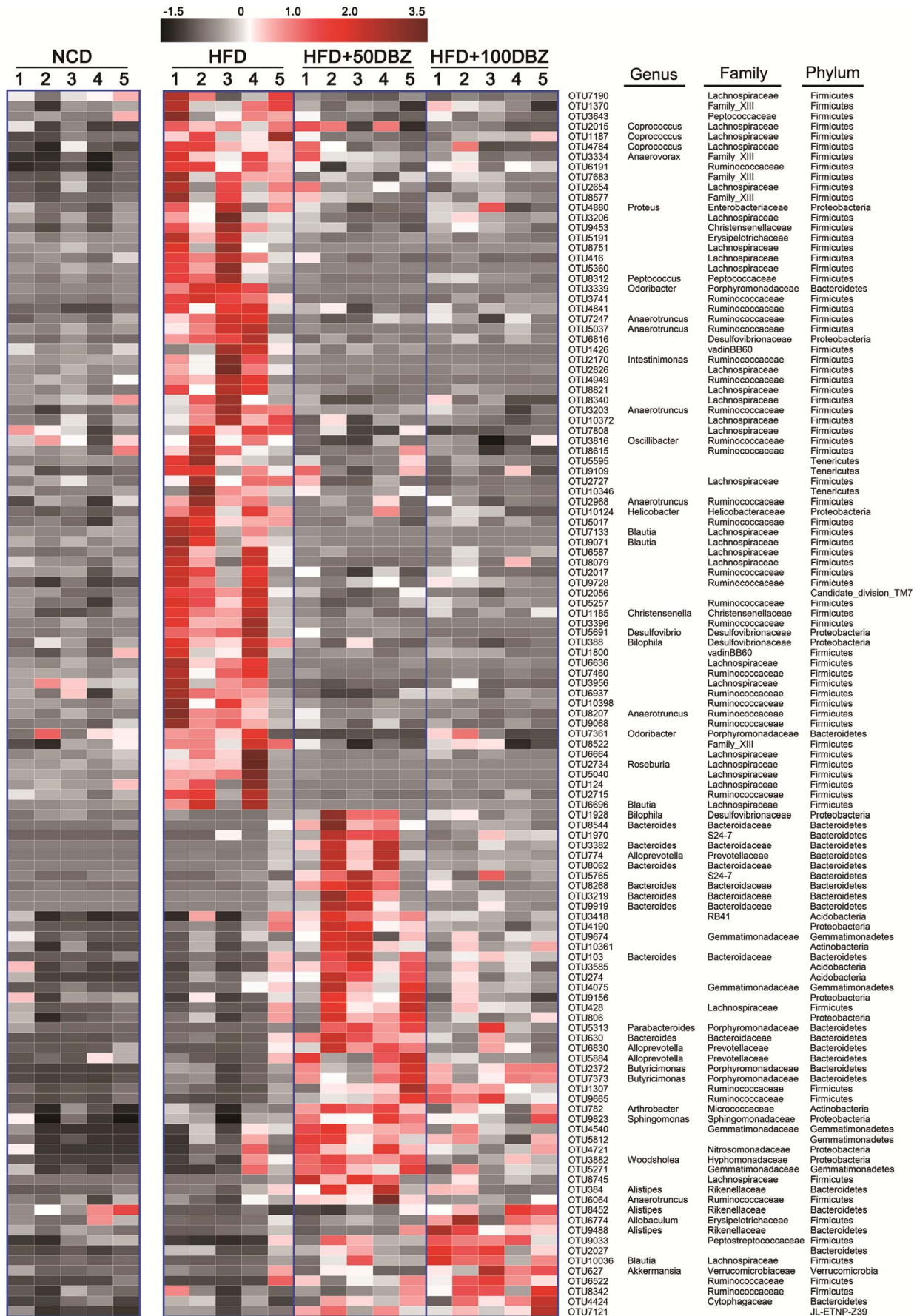


Fig. 6. DBZ alters the composition of the gut microbiota in HFD-fed mice. OTU-Venn (A) and Shannon curves and the Shannon index (B) of the gut microbiota in each group. Values are presented as the mean  $\pm$  SEM. \* $P < 0.05$  vs. NCD, # $P < 0.05$  vs. HFD. (C) PCoA score plot based on the Bray-Curtis analysis in each sample. The relative abundances of the gut microbiota at the phylum (D) and genus levels (E). The relative abundances of Akkermansia (F), Helicobacter marmotae (G), Odoribacter (H), and Anaerotruncus (I) obtained from the fecal microbiota are from the LEfSe results ( $P < 0.05$ ). The solid lines indicate the mean.



(caption on next page)

Fig. 7. Heatmap of 121 key OTUs responding to DBZ treatment in the HFD-fed mice. The color of the spot (left) corresponds to the standard score of the relative OTU abundance according to the RDA. The phylum, family and genus names of the OTUs are shown on the right ( $n = 5$ ).

the final manuscript.

### Transparency document

The Transparency document associated with this article can be found, in online version.

### Acknowledgments

We thank Professor Wen Xie for the critical reading of the manuscript, Professor Youfei Guan for supply of plasmids pCMX-PPAR $\gamma$  and PPRE  $\times$  3-TK-Luc, Professor Zhijie Chang for plasmid NF- $\kappa$ B-Luc, and Professor Nanping Wang for plasmids pCMX-PPAR $\alpha$  and pcDNA-hPPAR $\beta/\delta$ . This work was supported by the National Natural Science Foundation of China (no. 31571164 and no. 31271207) and Program for Innovative Research Team in Ministry of Education of China (IRT-15R55).

### Conflicts of Interest

The authors have declared that no competing interests exist. This project is supported by academic grants and there is no financial conflict of interest.

### Appendix A. Supplementary data

Supplementary data to this article can be found online at <http://dx.doi.org/10.1016/j.bbagen.2017.07.013>.

### References

- R.M. Evans, G.D. Barish, Y.X. Wang, PPARs and the complex journey to obesity, *Nat. Med.* 10 (2004) 355–361.
- M. Ahmadian, J.M. Suh, N. Hah, C. Liddle, A.R. Atkins, M. Downes, R.M. Evans, PPARgamma signaling and metabolism: the good, the bad and the future, *Nat. Med.* 19 (2013) 557–566.
- J. Auwerx, PPARgamma, the ultimate thrifty gene, *Diabetologia* 42 (1999) 1033–1049.
- R.E. Soccio, E.R. Chen, S.R. Rajapurkar, P. Safabakhsh, J.M. Marinis, J.R. Dispirito, M.J. Emmett, E.R. Briggs, B. Fang, L.J. Everett, H.W. Lim, K.J. Won, D.J. Steger, Y. Wu, M. Civelek, B.F. Voight, M.A. Lazar, Genetic variation determines PPARgamma function and anti-diabetic drug response in vivo, *Cell* 162 (2015) 33–44.
- J. Zhou, M. Febbraio, T. Wada, Y. Zhai, R. Kuruba, J. He, J.H. Lee, S. Khadem, S. Ren, S. Li, R.L. Silverstein, W. Xie, Hepatic fatty acid transporter Cd36 is a common target of LXR, PXR, and PPARgamma in promoting steatosis, *Gastroenterology* 134 (2008) 556–567.
- L. Wang, B. Waltenberger, E.M. Pferschy-Wenzig, M. Blunder, X. Liu, C. Malainer, T. Blazevic, S. Schwaiger, J.M. Rollinger, E.H. Heiss, D. Schuster, B. Kopp, R. Bauer, H. Stuppner, V.M. Dirsch, A.G. Atanasov, Natural product agonists of peroxisome proliferator-activated receptor gamma (PPARgamma): a review, *Biochem. Pharmacol.* 92 (2014) 73–89.
- A.G. Atanasov, J.N. Wang, S.P. Gu, J. Bu, M.P. Kramer, L. Baumgartner, N. Fakhrudin, A. Ladurner, C. Malainer, A. Vuorinen, S.M. Noha, S. Schwaiger, J.M. Rollinger, D. Schuster, H. Stuppner, V.M. Dirsch, E.H. Heiss, Honokiol: a non-adipogenic PPARgamma agonist from nature, *Biochim. Biophys. Acta* 1830 (2013) 4813–4819.
- P.J. Turnbaugh, R.E. Ley, M. Hamady, C.M. Fraser-Liggett, R. Knight, J.I. Gordon, The human microbiome project, *Nature* 449 (2007) 804–810.
- A. Bouchie, White house unveils national microbiome initiative, *Nat. Biotechnol.* 34 (2016) 580.
- J.K. Nicholson, E. Holmes, J. Kinross, R. Burcelin, G. Gibson, W. Jia, S. Pettersson, Host-gut microbiota metabolic interactions, *Science* 336 (2012) 1262–1267.
- S. Bashiardes, H. Shapiro, S. Rozin, O. Shibolet, E. Elinav, Non-alcoholic fatty liver and the gut microbiota, *Mol. Metab.* 5 (2016) 782–794.
- L.P. Zhao, The gut microbiota and obesity: from correlation to causality, *Nat. Rev. Microbiol.* 11 (2013) 639–647.
- J.C. Clemente, L.K. Ursell, L.W. Parfrey, R. Knight, The impact of the gut microbiota on human health: an integrative view, *Cell* 148 (2012) 1258–1270.
- A. Everard, V. Lazarevic, M. Derrien, M. Girard, G.M. Muccioli, A.M. Neyrinck, S. Possemiers, A. Van Holle, P. Francois, W.M. de Vos, N.M. Delzenne, J. Schrenzel, P.D. Cani, Responses of gut microbiota and glucose and lipid metabolism to prebiotics in genetic obese and diet-induced leptin-resistant mice, *Diabetes* 60 (2011) 2775–2786.
- M.A. Hildebrandt, C. Hoffmann, S.A. Sherrill-Mix, S.A. Keilbaugh, M. Hamady, Y.Y. Chen, R. Knight, R.S. Ahima, F. Bushman, G.D. Wu, High-fat diet determines the composition of the murine gut microbiome independently of obesity, *Gastroenterology* 137 (2009) 1716–1724.
- A. Woting, N. Pfeiffer, G. Loh, S. Klaus, M. Blaut, Clostridium ramosum promotes high-fat diet-induced obesity in gnotobiotic mouse models, *MBio* 5 (2014) e01530–01514.
- X. Xie, S. Wang, L. Xiao, J. Zhang, J. Wang, J. Liu, X. Shen, D. He, X. Zheng, Y. Zhai, DBZ blocks LPS-induced monocyte activation and foam cell formation via inhibiting nuclear factor- $\kappa$ B, *Cell. Physiol. Biochem.* 28 (2011) 649–662.
- X. Zhao, X. Zheng, T.P. Fan, Z. Li, Y. Zhang, J. Zheng, A novel drug discovery strategy inspired by traditional medicine philosophies, *Science* 347 (2015) S38–S40.
- J.Y. Han, J.Y. Fan, Y. Horie, S. Miura, D.H. Cui, H. Ishii, T. Hibi, H. Tsuneki, I. Kimura, Ameliorating effects of compounds derived from *Salvia miltiorrhiza* root extract on microcirculatory disturbance and target organ injury by ischemia and reperfusion, *Pharmacol. Ther.* 117 (2008) 280–295.
- J. Guo, Y. Yong, J. Aa, B. Cao, R. Sun, X. Yu, J. Huang, N. Yang, L. Yan, X. Li, J. Cao, N. Aa, Z. Yang, X. Kong, L. Wang, X. Zhu, X. Ma, Z. Guo, S. Zhou, H. Sun, G. Wang, Compound danshen dripping pills modulate the perturbed energy metabolism in a rat model of acute myocardial ischemia, *Sci Rep* 6 (2016) 37919.
- P. Xu, F. Hong, J. Wang, Y. Cong, S. Dai, S. Wang, J. Wang, X. Jin, F. Wang, J. Liu, Y. Zhai, Microbiome remodeling via the montmorillonite adsorption-excretion axis prevents obesity-related metabolic disorders, *EBioMedicine* 16 (2017) 251–261.
- L. Xiao, J. Wang, J. Li, X.W. Chen, P.F. Xu, S.Z. Sun, D.C. He, Y.S. Cong, Y.G. Zhai, ROR alpha inhibits adipocyte-conditioned medium-induced colorectal cancer cell proliferation and migration and chick embryo chorioallantoic membrane angiogenesis, *Am. J. Physiol. Cell Physiol.* 308 (2015) C385–C396.
- P.F. Xu, S. Dai, J. Wang, J. Zhang, J. Liu, F. Wang, Y.G. Zhai, Preventive obesity agent montmorillonite adsorbs dietary lipids and enhances lipid excretion from the digestive tract, *Sci Rep* 6 (2016) 19659.
- I. Toth, L. Fairall, K. Amin, Y. Inaba, A. Szanto, B.L. Balint, L. Nagy, K. Yamamoto, J.W. Schwabe, Structural basis for the activation of PPARgamma by oxidized fatty acids, *Nat. Struct. Mol. Biol.* 15 (2008) 924–931.
- T. Magoc, S.L. Salzberg, FLASH: fast length adjustment of short reads to improve genome assemblies, *Bioinformatics* 27 (2011) 2957–2963.
- A.M. Bolger, M. Lohse, B. Usadel, Trimmomatic: a flexible trimmer for Illumina sequence data, *Bioinformatics* 30 (2014) 2114–2120.
- R.C. Edgar, UPARSE: highly accurate OTU sequences from microbial amplicon reads, *Nat. Methods* 10 (2013) 996–998.
- J.G. Caporaso, J. Kuczynski, J. Stombaugh, K. Bittinger, F.D. Bushman, E.K. Costello, N. Fierer, A.G. Pena, J.K. Goodrich, J.I. Gordon, G.A. Huttley, S.T. Kelley, D. Knights, J.E. Koenig, R.E. Ley, C.A. Lozupone, D. McDonald, B.D. Muegge, M. Pirrung, J. Reeder, J.R. Sevinsky, P.J. Turnbaugh, W.A. Walters, J. Widmann, T. Yatsunenko, J. Zaneveld, R. Knight, QIIME allows analysis of high-throughput community sequencing data, *Nat. Methods* 7 (2010) 335–336.
- N. Segata, J. Izard, L. Waldron, D. Gevers, L. Miropolsky, W.S. Garrett, C. Huttenhower, Metagenomic biomarker discovery and explanation, *Genome Biol.* 12 (2011) R60.
- P.D. Cani, R. Bibiloni, C. Knauf, A. Waeg, A.M. Neyrinck, N.M. Delzenne, R. Burcelin, Changes in gut microbiota control metabolic endotoxemia-induced inflammation in high-fat diet-induced obesity and diabetes in mice, *Diabetes* 57 (2008) 1470–1481.
- Y. Kidani, S.J. Bensinger, Liver X receptor and peroxisome proliferator-activated receptor as integrators of lipid homeostasis and immunity, *Immunol. Rev.* 249 (2012) 72–83.
- K.I. Stanford, R.J. Middelbeek, K.L. Townsend, D. An, E.B. Nygaard, K.M. Hitchcox, K.R. Markan, K. Nakano, M.F. Hirshman, Y.H. Tseng, L.J. Goodyear, Brown adipose tissue regulates glucose homeostasis and insulin sensitivity, *J. Clin. Invest.* 123 (2013) 215–223.
- S. Beyaz, M.D. Mana, J. Roper, D. Kedrin, A. Saadatpour, S.J. Hong, K.E. Bauer-Rowe, M.E. Xifaras, A. Akkad, E. Arias, L. Pinello, Y. Katz, S. Shinagare, M. Abu-Remaileh, M.M. Mihaylova, D.W. Lamming, R. Dogum, G. Guo, G.W. Bell, M. Selig, G.P. Nielsen, N. Gupta, C.R. Ferrone, V. Deshpande, G.C. Yuan, S.H. Orkin, D.M. Sabatini, O.H. Yilmaz, High-fat diet enhances stemness and tumorigenicity of intestinal progenitors, *Nature* 531 (2016) 53–58.
- C.J. Chang, C.S. Lin, C.C. Lu, J. Martel, Y.F. Ko, D.M. Ojcius, S.F. Tseng, T.R. Wu, Y.Y. Chen, J.D. Young, H.C. Lai, *Ganoderma lucidum* reduces obesity in mice by modulating the composition of the gut microbiota, *Nat. Commun.* 6 (2015) 7489.
- P. Jia, S. Wang, C. Xiao, L. Yang, Y. Chen, W. Jiang, X. Zheng, G. Zhao, W. Zang, X. Zheng, The anti-atherosclerotic effect of tanshinol borneol ester using fecal metabolomics based on liquid chromatography-mass spectrometry, *Analyst* 141 (2016) 1112–1120.
- W. Lee, J. Ham, H.C. Kwon, Y.K. Kim, S.N. Kim, Anti-diabetic effect of amorpha-tibol through PPARalpha/gamma dual activation in db/db mice, *Biochem. Biophys. Res. Commun.* 432 (2013) 73–79.
- C. Weidner, J.C. de Groot, A. Prasad, A. Freivald, C. Quedenau, M. Kliem, A. Witzke, V. Kodolja, C.T. Han, S. Giegold, M. Baumann, B. Klebl, K. Siems, L. Muller-Kuhr, A. Schurmann, R. Schuler, A.F. Pfeiffer, F.C. Schroeder, K. Bussow, S. Sauer, Amorfrutins are potent antidiabetic dietary natural products, *Proc. Natl.*

- Acad. Sci. U. S. A. 109 (2012) 7257–7262.
- [38] C. Weidner, S.J. Wowro, A. Freiwald, K. Kawamoto, A. Witzke, M. Kliem, K. Siems, L. Muller-Kuhr, F.C. Schroeder, S. Sauer, Amorfrutin B is an efficient natural peroxisome proliferator-activated receptor gamma (PPAR gamma) agonist with potent glucose-lowering properties, *Diabetologia* 56 (2013) 1802–1812.
- [39] E.P. Mottillo, E.M. Desjardins, J.D. Crane, B.K. Smith, A.E. Green, S. Ducommun, T.I. Henriksen, I.A. Rebalka, A. Razi, K. Sakamoto, C. Scheele, B.E. Kemp, T.J. Hawke, J. Ortega, J.G. Granneman, G.R. Steinberg, Lack of adipocyte AMPK exacerbates insulin resistance and hepatic steatosis through brown and beige adipose tissue function, *Cell Metab.* 24 (2016) 118–129.
- [40] G. Hoeke, S. Kooijman, M.R. Boon, P.C. Rensen, J.F. Berbee, Role of brown fat in lipoprotein metabolism and atherosclerosis, *Circ. Res.* 118 (2016) 173–182.
- [41] P. Xu, J. Wang, F. Hong, S. Wang, X. Jin, T. Xue, L. Jia, Y. Zhai, Melatonin prevents obesity through modulation of gut microbiota in mice, *J. Pineal Res.* 4 (2017) 12399.
- [42] C. Wang, X. Zeng, Z. Zhou, J. Zhao, G. Pei, beta-arrestin-1 contributes to brown fat function and directly interacts with PPARalpha and PPARgamma, *Sci Rep* 6 (2016) 26999.
- [43] L. Miele, G. Marrone, C. Lauritano, C. Cefalo, A. Gasbarrini, C. Day, A. Grieco, Gut-liver axis and microbiota in NAFLD: insight pathophysiology for novel therapeutic target, *Curr. Pharm. Des.* 19 (2013) 5314–5324.
- [44] H. Tilg, A.R. Moschen, Microbiota and diabetes: an evolving relationship, *Gut* 63 (2014) 1513–1521.
- [45] N.R. Shin, J.C. Lee, H.Y. Lee, M.S. Kim, T.W. Whon, M.S. Lee, J.W. Bae, An increase in the *Akkermansia* spp. population induced by metformin treatment improves glucose homeostasis in diet-induced obese mice, *Gut* 63 (2014) 727–735.
- [46] S. Lukovac, C. Belzer, L. Pellis, B.J. Keijsers, W.M. de Vos, R.C. Montijn, G. Roeselers, Differential modulation by *Akkermansia muciniphila* and *Faecalibacterium prausnitzii* of host peripheral lipid metabolism and histone acetylation in mouse gut organoids, *MBio* 5 (2014) e01438–01414.
- [47] H. Plovier, A. Everard, C. Druart, C. Depommier, M. Van Hul, L. Geurts, J. Chilloux, N. Ottman, T. Duparc, L. Lichtenstein, A. Myridakis, N.M. Delzenne, J. Klievink, A. Bhattacharjee, K.C. van der Ark, S. Aalvink, L.O. Martinez, M.E. Dumas, D. Maiter, A. Loumaye, M.P. Hermans, J.P. Thissen, C. Belzer, W.M. de Vos, P.D. Cani, A purified membrane protein from *Akkermansia muciniphila* or the pasteurized bacterium improves metabolism in obese and diabetic mice, *Nat. Med.* 23 (2017) 107–113.
- [48] M.C. Collado, E. Isolauri, K. Laitinen, S. Salminen, Distinct composition of gut microbiota during pregnancy in overweight and normal-weight women, *Am. J. Clin. Nutr.* 88 (2008) 894–899.
- [49] A. Everard, C. Belzer, L. Geurts, J.P. Ouwerkerk, C. Druart, L.B. Bindels, Y. Guiot, M. Derrien, G.G. Muccioli, N.M. Delzenne, W.M. de Vos, P.D. Cani, Cross-talk between *Akkermansia muciniphila* and intestinal epithelium controls diet-induced obesity, *Proc. Natl. Acad. Sci. U. S. A.* 110 (2013) 9066–9071.
- [50] P.D. Cani, J. Amar, M.A. Iglesias, M. Poggi, C. Knauf, D. Bastelica, A.M. Neyrinck, F. Fava, K.M. Tuohy, C. Chabo, A. Waget, E. Delmee, B. Cousin, T. Sulpice, B. Chamontin, J. Ferrieres, J.F. Tanti, G.R. Gibson, L. Casteilla, N.M. Delzenne, M.C. Alessi, R. Burcelin, Metabolic endotoxemia initiates obesity and insulin resistance, *Diabetes* 56 (2007) 1761–1772.
- [51] M.M. Patterson, A.B. Rogers, J.G. Fox, Experimental helicobacter marmotae infection in A/J mice causes enterohepatic disease, *J. Med. Microbiol.* 59 (2010) 1235–1241.
- [52] A. Everard, S. Matamoros, L. Geurts, N.M. Delzenne, P.D. Cani, *Saccharomyces boulardii* administration changes gut microbiota and reduces hepatic steatosis, low-grade inflammation, and fat mass in obese and type 2 diabetic db/db mice, *MBio* 5 (2014) e01011–01014.